Light-Driven Rapid Peeling of Photochromic Diarylethene Single Crystals

Masato Tamaoki, Daichi Kitagawa, Seiya Kobatake

概　要	研究グループは、紫外線や可視光線を照射すると色が変化するフォトクロミック化合物からなる結晶に紫外線を照射することで、世界最速で適切な大きさの結晶（フォトアクチュエーター素子）を剥離することに成功しました。 研究グループはこれまでジアリールエテンと呼ばれる化合物からなる結晶のフォトメカニカル挙動に関する研究を行っており、光を照射することで分子の構造を変化させ、結晶の伸縮、屈曲、ねじれなどの挙動を見出してきました※。このような結晶はマイクロメートルサイズの微小な結晶であり、次世代の微小な領域におけるフォトアクチュエーターとしての応用が期待されています。しかしながら、屈曲などの挙動は結晶のサイズに依存するため、適切なサイズの結晶を作り分けることが課題となっていました。 そこでフォトクロミック化合物から構成される結晶に紫外線を照射したところ、世界最速でフォトアクチュエーター素子を剥離させることに成功しました。これまでフォトメカニカル挙動を示さない大きな結晶は使用できませんでしたが、本手法により、大きな結晶でもマイクロメートルサイズの適切な大きさにカットして使用でき、非常に高速な屈曲挙動も可能になりました。 ‘紫外線でフォトメカニカル有機結晶を世界最速で剥離’. 大阪市立大学. https://www.osaka-cu.ac.jp/ja/news/2021/210419. (参照 2021-04-20) ※ ‘世界初！ 光をあてるとさまざまな形に変形する結晶を発見!!’. 大阪市立大学. https://www.osaka-cu.ac.jp/ja/news/2017/180219-2. (参照 2021-04-20)
関連情報	「Crystal Growth & Design」誌の表紙を飾りました。 https://www.osaka-cu.ac.jp/ja/news/2021/210510

Light-driven Rapid Peeling of Photochromic Diarylethene Single Crystals

Masato Tamaoki, Daichi Kitagawa, and Seiya Kobatake*

Department of Applied Chemistry, Graduate School of Engineering Osaka City University, 3-3-138 Sugimoto, Sumiyoshi-ku, Osaka 558-8585, Japan

KEYWORDS. Photomechanical; Photochromism; Diarylethene; Organic Crystal; Photosalient

ABSTRACT: Macroscopic transformation such as the molecular motors of biology is brought by transforming the protein using the chemical reaction of molecules by external stimuli. If it is possible to achieve it as machine-like in nanometer to micrometer size in photomechanical phenomena, there is a possibility of the application as driving devices of micro- or nano-machineries that drive without any electrical contact. Since light is useful to operate it without any direct contact as external stimuli and leads to rapid photochemical reactions, the operation at high speed can be expected. Here we newly found that crystals of a photochromic diarylethene exhibit a peeling behavior with astonishingly rapid velocity by photoirradiation to a lateral face in addition to separation behaviors such as jumping and cracking by photoirradiation to a well-developed face. The detail of the rapid photoresponsive peeling was discussed based on the molecular packings and the dependence on crystal size and photoirradiation conditions. These crystals can be potentially applied to macroscopic photomechanical actuators rapidly driven based on molecular machinery.

INTRODUCTION

Photomechanical crystals that show mechanical motions by photoirradiation is one of the most rapidly developing research fields in crystal chemistry, material chemistry, and photochemistry.[1,2] Photomechanical motions are induced by the accumulation of very small changes in molecular structure due to photochemical reactions in the crystal. In other words, the release of strain caused by the photochemical reactions results in mechanical motions. As a result of efforts by many researchers, various photomechanical behaviors of the crystals have been reported so far such as expansion, contraction, bending, twisting, coiling, sweeping, jumping, cracking, and peeling.[3-21] Among these photomechanical behaviors, the bending behavior is the most common motion and the detailed investigation for the bending motion has been performed. It has been revealed that the crystal thickness, length, aspect ratio, and the rates of forward and reverse reactions as intrinsic factors and the temperature, exposure time, and irradiation power as extrinsic factors affect the bending behavior.[22-27] Furthermore, several mathematical models were developed to quantitatively evaluate the bending motion.[28-30]

On the other hand, there are only two examples of the peeling behavior,[20,21] meaning that the peeling is a very rare motion. It is not clear what is the difference between the peeling behavior and other behaviors. To address this issue, there are two possible ways. One is to find molecules that exhibit a peeling behavior and other behaviors depending on polymorphism. X-ray crystallographic analysis would reveal the relationship between the photomechanical behaviors and the molecular packings in crystals. The other is to discover a molecular crystal showing both a peeling behavior and other behaviors depending on the factors such as crystal size and photoirradiation conditions. The dependence of the peeling behavior on some factors would provide useful information to discuss the detailed mechanism of the peeling behavior.

Our group has been investigating the photomechanical behavior of photochromic diarylethene crystals that undergo ring-cyclization and ring-opening reactions by alternating irradiation with ultraviolet (UV) light and visible light. Fortunately, in this study, we found that crystals of a diarylethene having a styrene skeleton at one end (**1a** in Figure 1) exhibit a peeling behavior in addition to a separation shearing behavior such as jumping and cracking. Here we report on the details of the photomechanical peeling and separation shearing behaviors of single crystal **1a**. In particular, the dependence of the peeling behavior on the crystal size and photoirradiation conditions was examined in detail.

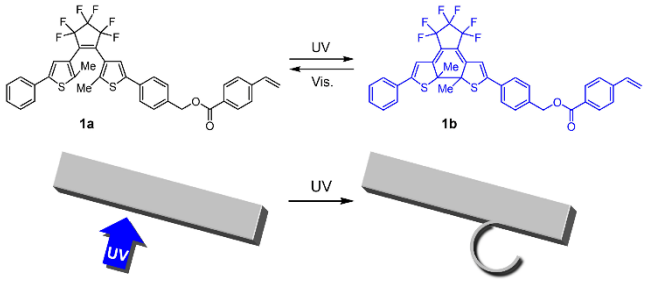

Figure 1. Photochromic reactions of **1a** and illustration of light-driven peeling behavior.

RESULTS AND DISCUSSION

Characterization of crystal 1a. When recrystallized from *n*-hexane/acetone solution, single crystals of **1a** can be obtained as shown in Figure 2a. The crystals had a length of 300 to 1600 μm, a width of 50 to 150 μm, and a thickness of 10 to 40 μm.

There are eight faces on the crystal. To investigate the molecular packing in the crystal, a single-crystal X-ray diffraction measurement of **1a** was performed, as summarized in Table S1. The crystal system and space group of crystal **1a** were monoclinic and $P2_1/c$, respectively. Crystal **1a** consists of four diarylethene molecules in the unit cell and one diarylethene molecule in the asymmetric unit. All the diarylethene molecules are fixed in a photoreactive antiparallel conformation, and the distance between the reactive carbon atoms is 0.359 nm, which is short enough to undergo photocyclization in the crystalline phase (Figure 2b).[31]

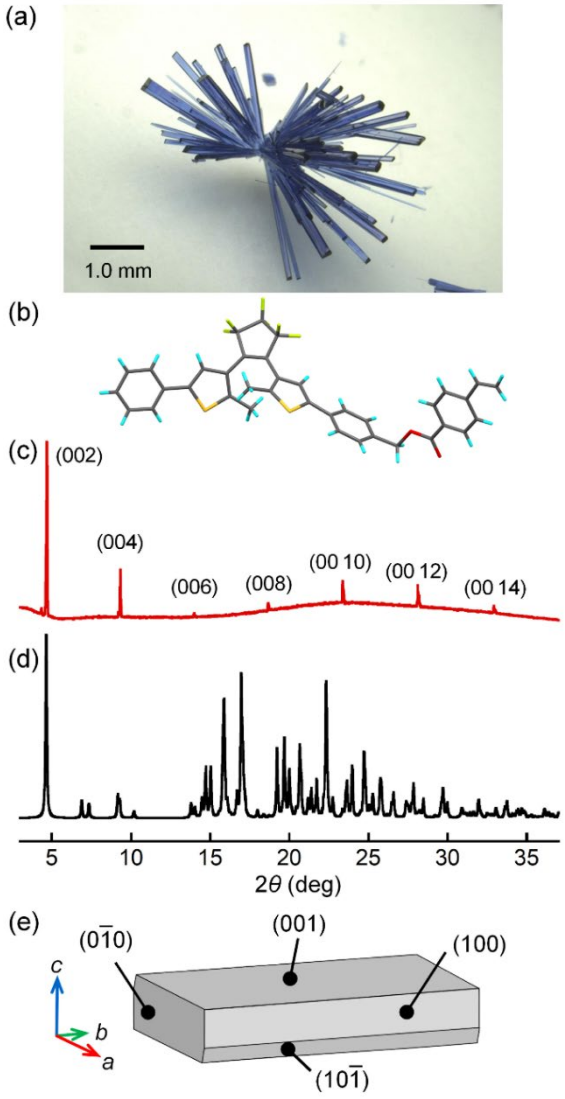

Figure 2. (a) Optical microphotograph of single crystals of **1a** (The crystals were slightly colored by UV irradiation). (b) Molecular structure of **1a** in the crystal determined by X-ray crystallographic analysis. (c) PXRD pattern of crystal **1a** on the well-developed face of the crystals and (d) the pattern calculated from X-ray crystallographic analysis of single crystal **1a**. (e) Crystal shape and face indices predicted by BFDH rule.

To identify the molecular orientation in the crystal, powder X-ray diffraction (PXRD) measurement was done. Figure 2c,d show a PXRD pattern on the well-developed face of the single crystals and the pattern calculated from single-crystal X-ray crystallographic data of crystal **1a**, respectively. As shown in Figure 2c, only diffraction peaks originating from the (001) plane were observed for the face of crystal **1a**, meaning that the well-developed face of the crystal can be assigned to the (001) plane. To get more information about the molecular orientation in the plane, the crystal shape was predicted using a Bravais-Friedel-Donnay-Harker (BFDH) analysis,[32-35] as shown in Figure 2e. The predicted crystal shape has the (001), (100), (10$\bar{1}$), and (0$\bar{1}$0) planes. The PXRD pattern of the slightly crushed crystal **1a** points out the existence of the (101) plane, as shown in Figure S1. The actual crystals have the (101) plane, as can be seen from Figure 6.

When the (001) plane was irradiated with 365 nm light for a few seconds, the crystal color changed from colorless to blue due to the photochromic reaction from **1a** to **1b** in the crystal. The absorption maximum appeared at 575 nm. When the colored crystal was observed under polarized light, the absorption intensity was almost the same in the changing polarization directions of 0 and 90° as shown in Figure S2c,d. This is ascribed to the molecular orientation that is perpendicular to each other.[36] Thus, the molecular orientation in the crystal was fully characterized.

The photoirradiated colored crystals were dissolved in *n*-hexane to confirm that the only reversible photochromic reaction occurs and the styryl group does not react in the crystal of **1a**. The only open- and closed-ring isomers were detected by a high-performance liquid chromatography (HPLC). This indicates that any photoreactions of the styryl group are prohibited in the crystal.

Photomechanical response of crystal 1a. Interestingly, we found that crystals **1a** exhibited a photoinduced rapid peeling behavior when exposed to 365 nm light on the lateral face of the crystal as shown in Figures 3,S3 and Videos S1-S3 (high-speed camera). There is an induction time before the peeling occurs and it takes only 175 microseconds from the start to the end of the peeling behavior. This is very fast compared with the peeling behaviors reported previously that take tens of seconds and tens of minutes.[20,21] The peeling behavior occurred multiple times from the same parent crystal, but tended not to occur after a while, which might be due to the light filtering effect of the closed-ring form.

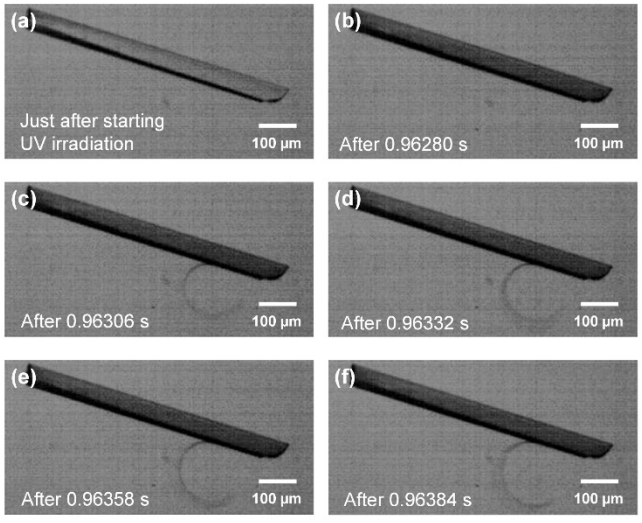

Figure 3. Photoinduced rapid peeling of a diarylethene single crystal of **1a** taken by a high-speed camera (black and white). The crystal color turned from colorless to blue by irradiation with 365 nm light. See Videos S1 and S2 in Supporting Information.

Figure 4 shows crystal winding by peeling upon irradiation with 365 nm light. The horizontal speed and rotation speed during the winding of the peeling crystal were estimated to be 2.4 m s^{-1} and 8000 rps, respectively. Such high-speed winding results from large strains caused by the photochromic reaction.

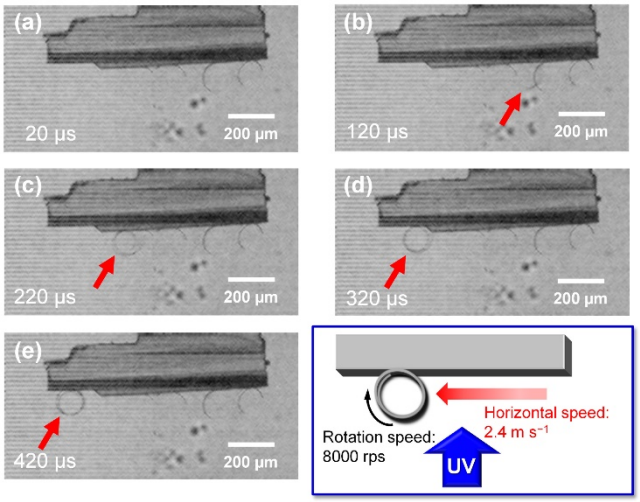

Figure 4. Photoinduced rapid peeling and winding of crystal **1a**. The time at the bottom left shows time from a certain time. The red arrows indicate the location of the crystal peeling and winding. See Video S4 in Supporting Information.

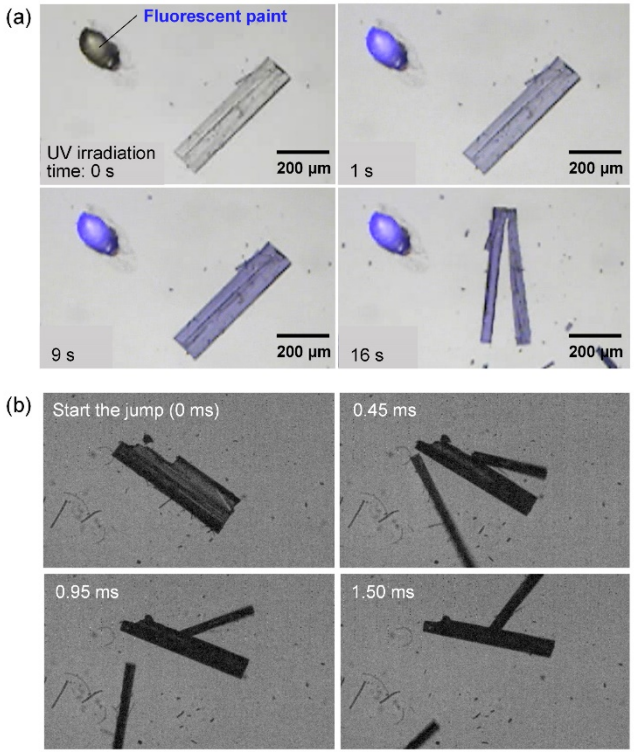

Figure 5. (a) Separation shearing and (b) jumping of crystal **1a** upon irradiation with 365 nm light to the well-developed face. See Videos S5, S6 for photoinduced rapid separation shearing (real-time movie) and jumping (black and white in high-speed camera) in Supporting Information.

Next, we investigated the photomechanical response of crystal **1a** upon irradiation to well-developed face. Upon irradiation with 365 nm light on the (001) plane of crystal **1a**, the crystals exhibited cracking and jumping with some extent induction period as shown in Figure 5 and Videos S5, S6. These behaviors are called "separation shearing behavior" and known as the phenomenon ascribed to the quick release of the strain induced by photoreactions in the crystal.[37] This is because the crystal size is too large to deform for the release of the strain.

Mechanism of the photomechanical response. Here we have a simple question why the photomechanical behavior, separation shearing or peeling, depends on the irradiated face of the crystal. To address this issue, the cross-section of the crystal viewed from the $(0\bar{1}0)$ plane was observed before and after irradiation with UV light as shown in Figure 6a,b. As can be seen from the molecular packing, after separation shearing, the corner angle of the crystal viewed from cross-section was 104° (Figure 6a). Moreover, that for the peeling was also 104° as shown in Figure 6b. Thus, both cross-section angles of the separation shearing and the peeling were the same. To know the meaning of this specific angle of 104°, the molecular packing was viewed from the $(0\bar{1}0)$ plane as shown in Figure 6c. There is a possible plane to cleave along the $(10\bar{1})$ plane (i.e. the gap between molecules) that has the dihedral angle of 104° with the (001) plane. This result clearly indicates that the cracking takes place along the $(10\bar{1})$ plane.

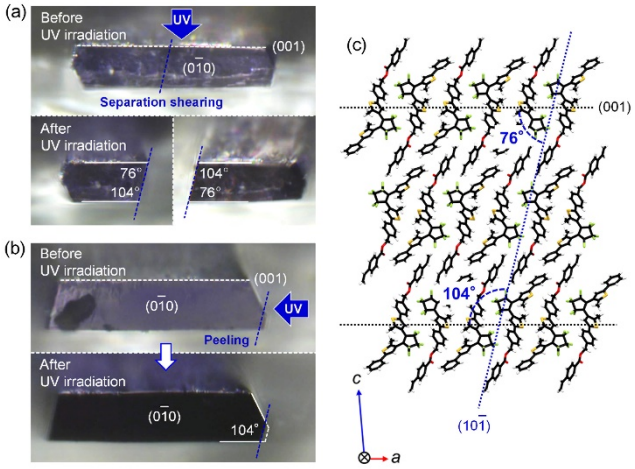

Figure 6. Optical microphotographs of the cross-section of crystal **1a** viewed from the $(0\bar{1}0)$ plane before and after (a) the separation shearing and (b) the peeling upon UV irradiation. (c) Molecular packing of **1a** viewed from the $(0\bar{1}0)$ plane.

Based on the observation of the cross-section of the crystal, we concluded the mechanism of the separation shearing and photoinduced peeling behaviors as shown in Figure 7a,b. When

UV irradiation was done to the (001) plane, the entire crystal exhibited photochromism from colorless to blue as shown in Figure 7a. Therefore, strain was generated in the entire crystal and the cracking occurred along the $(10\bar{1})$ plane to release the strain. On the other hand, when the lateral narrow surface was irradiated with UV light, the photochromic reaction takes place only in the vicinity of the irradiated surface of the crystal as shown in Figure 7b. Therefore, the strain was generated only in the vicinity of the irradiated surface, which results in peeling along the $(10\bar{1})$ plane.

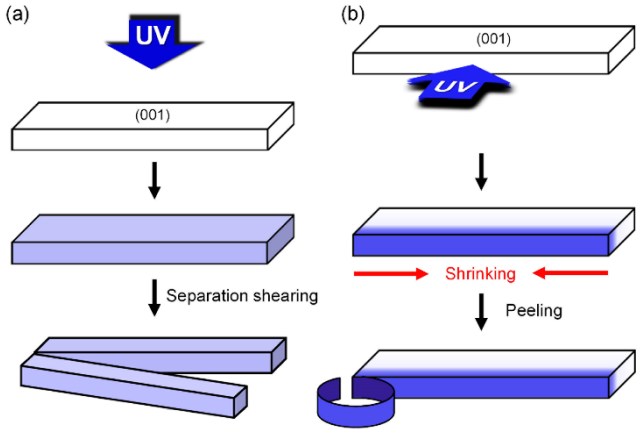

Figure 7. Schematic illustration of photomechanical behaviors of crystal **1a** upon irradiation with UV light to (a) the (001) plane and (b) the lateral narrow face.

To identify the crystallinity of the component delaminated from the parent crystal (hereafter denoted as "peel"), the birefringence was investigated using a polarized optical microscope. Figure S4 shows the optical microphotographs of the peel and the parent crystal of **1a** under crossed Nicols. The peel was bright under crossed Nicols as well as the parent crystal, meaning that the crystallinity is maintained even after peeling. In the previous study reported by Bardeen *et al.*, the experiment was carried out in solution and the component peeled off became amorphous due to the presence of the surfactant of sodium dodecylsulfate that enables the component to show a clean and slow detachment.[20] On the other hand, in our case, the experiment was performed in air, which would result in the rapid peeling behavior with maintaining the crystallinity.

To clarify the conversion ratio from the open-ring isomer to the closed-ring isomer in the peel, the peels generated from one crystal were collected and analyzed by HPLC. As a result of the analysis, the conversion in the peels was 16–28% as shown in Figure S5. This provides evidence that the photoisomerization does not proceed to 100% completion but instead reaches a conversion ratio enough to peel the crystal.

Dependence of the peeling behavior on various factors. To reveal the peeling behavior in more detail, the relationships between the peeling behavior and various factors were investigated. First, the dependence of the peeling behavior on crystal size was investigated. Definitions of crystal length, width, thickness, induction period, curvature, and thickness of peel are shown in Figure S6. The induction period represents time from start of UV irradiation to start of peeling. The relationships between the induction period and the crystal length, crystal width, and crystal thickness are shown in Figure 8a. As can be seen from these three graphs, the induction period is in the range of 3 to 6 s and is independent of crystal length, crystal width, and crystal thickness. Similarly, the curvature and thickness of peel relative to crystal length, crystal width, and crystal thickness are shown in Figures 8b,c. They are also in a certain range as well as that for the induction period and are also independent of the crystal length, the crystal width, and the crystal thickness. Based on these results, it was revealed that the peeling behavior in this work has no dependence on the crystal size.

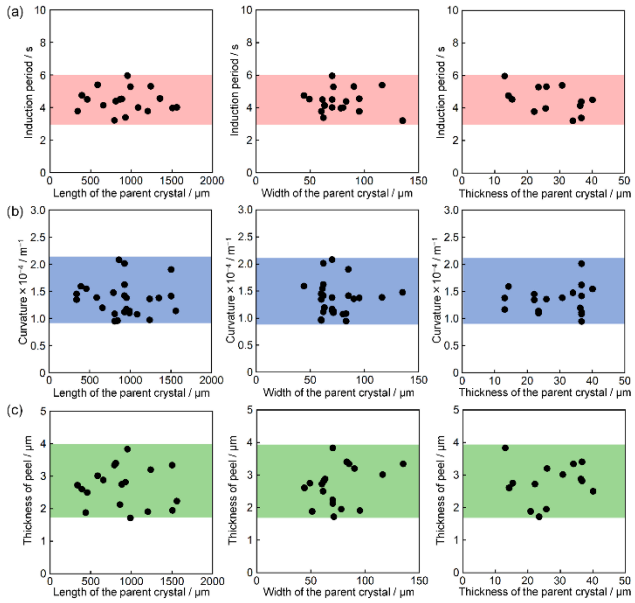

Figure 8. Dependence of the peeling behavior on various factors: (a) Induction period, (b) curvature, and (c) thickness of peel relative to length, width, and thickness of the parent crystal upon irradiation with 365 nm light.

Next, the dependence of the induction period on the irradiation intensity of the incident light was investigated as shown in Figure 9a. When the irradiation intensity increased, the induction period became shorter regardless of the irradiation wavelength. The irradiation intensity and the induction period have an inverse relationship, suggesting that when the reaction ratio in the photoirradiated crystal surface reaches a certain value, the peeling takes place to relax the strain in the crystal. Moreover, comparing the induction period with the irradiation wavelength at the same photon number, the induction period became shorter by irradiation of shorter wavelengths. This is due to the difference in the absorption of the crystal at the different irradiation wavelengths. As can be seen from the diffuse reflectance absorption spectrum of power crystals of 1a, the absorbance increases in the order of 380, 365, and 313 nm (Figure S7). As can be seen from Figure 9b, the curvature of the peel became larger when the irradiation wavelength is shorter, while it is independent of the irradiation intensity. Moreover, the thickness of the peel became thinner when the irradiation wavelength is shorter (Figure 9c).

Summing up the results described above, the peeling mechanism can be explained as shown in Figure 9d. Upon irradiation with a shorter wavelength light, a large amount of the incident light is absorbed in the vicinity of the crystal surface because the absorbance of **1a** in the shorter wavelength region is larger than that in the longer wavelength region as shown in Figure S7. Therefore, the photochromic reaction occurs only in the vicinity of the crystal surface and the strain is generated at a shallow position, which results in a thin peel with a large curvature. On the other hand, the incident light can penetrate relatively inside the crystal when the longer wavelength light was used for the irradiation. Then, photoisomerization also takes place inside the crystal and the strain is generated at a deep position. Therefore, a thick peel with a small curvature is generated.

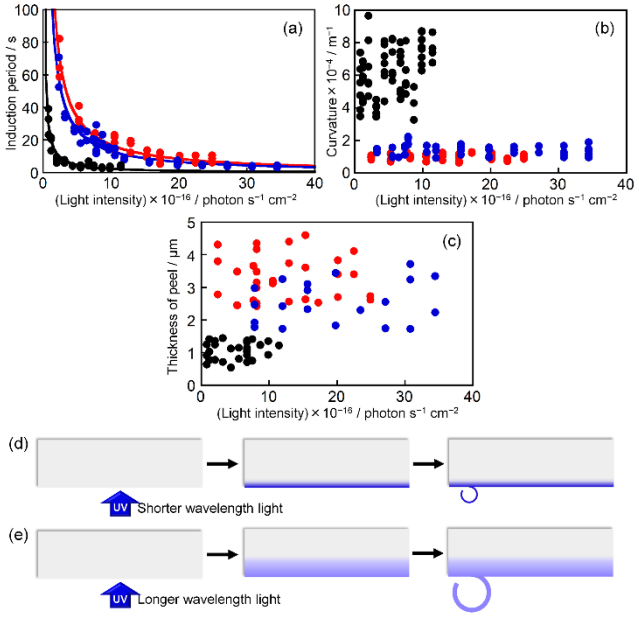

Figure 9. (a) Induction period, (b) curvature, and (c) thickness of the peel relative to irradiation intensity with 313 nm (black), 365 nm (blue), 380 nm (red) light. The difference in the peel upon irradiation with (d) shorter wavelength light and (e) longer wavelength light.

Photomechanical response of the peel. Finally, we have demonstrated the photomechanical behavior of the peel itself. The peel eliminated from the parent crystal was placed on a slide glass and irradiated with visible light to form colorless crystal with straight shape as shown in Figure S8. Then, upon irradiation with high-power 365 nm light (1.39 W cm^{-2}) focused by an objective lens for 0.5 s, the peel showed a quick photoinduced bending as shown in Figure 10 and Video S4. Interestingly, the curvature of the bent crystal was almost the same (1.25×10^4 m^{-1}) as that of the peel from the parent crystal. The total number of photons irradiated for 0.5 s was calculated to be 1.27×10^{18} photon cm^{-2}, which was almost the same number as that for the peeling behavior (ca. 1.33×10^{18} photon cm^{-2} which is averaged from Figure 9a). The photoreversible bending of the peel can be repeated many times. This result suggests that the peeling behavior described above is caused by the strain accumulated by the photocyclization reaction upon UV irradiation.

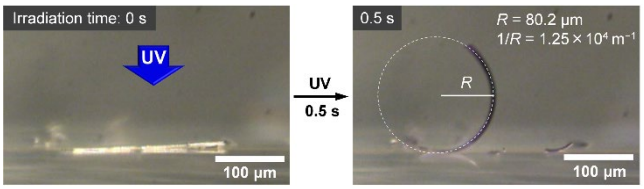

Figure 10. High-power radiation induced bending of the peel upon irradiation with 365 nm light of the same number of photons as that for the peeling behavior. See Video S7 in Supporting Information.

CONCLUSION

We investigated the photomechanical behavior of diarylethene crystals of **1a** upon UV irradiation. Upon irradiation to the wide face of the crystal, crystals exhibited jumping and cracking known as a separation shearing behavior, while the peeling behavior was observed when the lateral surface of the **1a** crystal was irradiated. Based on the investigation of the relationship between the molecular packing and the corner angles of the crystal viewed from the cross-section before and after the cracking, it was revealed that there is a plane to cleave along the crystal long axis. Thus, the separation shearing behavior with cracking occurs to release accumulated strain when relatively the entire crystal has reacted. On the other hand, when only the vicinity of the crystal surface reacts, a thin crystal can be peeled off along the plane to cleave. Moreover, it was clarified that the relationship between the UV irradiation intensity and the induction period is inversely proportional, which means that the peeling behavior takes place when a certain amount of strain is accumulated. Furthermore, it was found that the thickness and curvature of the peel can be controlled by modulating the irradiation wavelength. The photoinduced peeling of the crystal in this work and the photoinduced bending of the resulting peel crystal are extremely fast. These behaviors would be determined by a balance of the strain accumulated by the photochemical reaction, the intermolecular interaction of the molecules in the crystal, and the solid-state crystal properties. These results suggest that this finding provides the effective method for the fabrication of crystals with the optimum size showing rapid photoreversible bending behavior.

EXPERIMENTAL SECTION

General. Single crystal X-ray diffraction measurement was carried out using a Rigaku VariMax with Saturn CCD with MoK_α radiation (λ = 0.71073 Å) monochromated by graphite. The crystal structures were solved by a direct method using SIR92 and refined by the full matrix least-squares method on F^2 with anisotropic displacement parameters for non-hydrogen atoms using SHELXL-2014. Powder X-ray diffraction (PXRD) measurement was carried out using a Rigaku MiniFlex600. Polarized absorption spectra of crystal **1a** were measured using a Nikon ECLIPSE E600POL polarizing optical microscope equipped with a Hamamatsu PMA-11 photonic multichannel analyzer as the photodetector. Photoirradiation was carried out using a 100 W mercury lamp as a light source. Monochromatic light (365 nm light) was obtained by passing the light through a band-pass filter. The photomechanical behavior of crystals **1a** was observed using a Keyence VHX-500 digital microscope or a Nikon ECLIPSE TE2000-U inverted optical microscope equipped with a Phantom V12 high speed camera. UV irradiation was performed using a Keyence UV-LED UV-400/UV-

50H (365 nm light). UV irradiation power was measured using a Neoark PM-335A power meter. Crystal shape and face indices were predicted by WinXMorph.[35]

Material. Diarylethene **1a** was synthesized according to the procedures reported previously.[38]

Calculation of the photon number irradiated to the peel. The photon number irradiated to the samples can be calculated using the following equation:

$$E = n\,h\,c/\lambda$$

where E is the accumulated energy (J cm^{-2}) of the incident light until the bending of the peel was completed, n is the photon number (photon cm^{-2}), h is Planck's constant (6.626×10^{-34} J s), c is the speed of light (3.0×10^{8} m s^{-1}), and λ is the irradiation wavelength (365×10^{-9} m).

The E value can be obtained from the product of the irradiation intensity and the irradiation time. Here we should note that the peel is very small. Therefore, we accurately examined the irradiation intensity considering the distribution of the irradiation intensity within the beam. To know the intensity distribution of the beam, the fluorescent paper was irradiated with UV light from the left side (Figure S9a,b) under the same conditions as the photoinduced bending experiment in Figure 10, and a picture of the fluorescent paper was taken as shown in Figure S9c. The graph of the irradiation intensity relative to the distance from the beam center was prepared based on the intensity distribution obtained from the image and the total UV light intensity (3.93×10^{-2} W) (Figure S9d). Since the length of the peel was about 250 μm, the average irradiation intensity in the range of 125 μm from the beam center was calculated to be 1.39 W cm^{-2}. Then, the E value was estimated to be 0.693 J cm^{-2} as calculated from 1.39 W cm^{-2} × 0.5 s.

ASSOCIATED CONTENT

Supporting Information. The Supporting Information is available free of charge on the ACS Publications website. Detailed experimental data (Figures S1−S9 and Table S1) (PDF) and Videos S1−S7.

AUTHOR INFORMATION

Corresponding Author

* E-mail: kobatake@a-chem.eng.osaka-cu.ac.jp

ORCID

Daichi Kitagawa: 0000-0002-1994-3047
Seiya Kobatake: 0000-0002-1526-4629

Notes

The authors declare no competing financial interests.

Author Contributions

The manuscript was written through contributions of all authors. All authors have given approval to the final version of the manuscript.

ACKNOWLEDGMENT

The authors thank Nippon Zeon Co., Ltd. for providing octafluorocyclopentene.

REFERENCES

(1) White, T. J. *Photomechanical Materials, Composites, and Systems: Wireless Transduction of Light into Work*, John Wiley & Sons, 2017.

(2) Naumov, P.; Karothu, D. P.; Ahmed, E.; Catalano, L.; Commins, P.; Halabi, J. M.; Al-Handawi, M. B.; Li, L. The Rise of the Dynamic Crystals. *J. Am. Chem. Soc.* **2020**, *142*, 13256-13272.

(3) Kobatake, S.; Takami, S.; Muto, H.; Ishikawa, T.; Irie, M. Rapid and Reversible Shape Changes of Molecular Crystals on Photoirradiation. *Nature* **2007**, *446*, 778-781.

(4) Al-Kaysi, R. O.; Müller, A. M.; Bardeen, C. J. Photochemically Driven Shape Changes of Crystalline Organic Nanorods. *J. Am. Chem. Soc.* **2006**, *128*, 15938-15939.

(5) Al-Kaysi, R. O.; Bardeen, C. J. Reversible Photoinduced Shape Changes of Crystalline Organic Nanorods. *Adv. Mater.* **2007**, *19*, 1276-1280.

(6) Koshima, H.; Ojima, N.; Uchimoto, H. Mechanical Motion of Azobenzene Crystals upon Photoirradiation. *J. Am. Chem. Soc.* **2009**, *131*, 6890-6891.

(7) Bushuyev, O. S.; Tomberg, A.; Friščić, T.; Barrett, C. J. Shaping Crystals with Light: Crystal-to-Crystal Isomerization and Photomechanical Effect in Fluorinated Azobenzenes. *J. Am. Chem. Soc.* **2013**, *135*, 12556-12559.

(8) Bushuyev, O. S.; Singleton, T. A.; Barrett, C. J. Fast, Reversible, and General Photomechanical Motion in Single Crystals of Various Azo Compounds Using Visible Light. *Adv. Mater.* **2013**, *25*, 1796-1800.

(9) Koshima, H.; Ojima, N. Photomechanical Bending of 4-Aminoazobenzene Crystals. *Dyes Pigm.* **2012**, *92*, 798-801.

(10) Zhu, L.; Al-Kaysi, R. O.; Bardeen, C. J. Reversible Photoinduced Twisting of Molecular Crystal Microribbons. *J. Am. Chem. Soc.* **2011**, *133*, 12569-12575.

(11) Kitagawa, D.; Tsujioka, H.; Tong, F.; Dong, X.; Bardeen, C. J.; Kobatake, S. Control of Photomechanical Crystal Twisting by Illumination Direction. *J. Am. Chem. Soc.* **2018**, *140*, 4208-4212.

(12) Kitagawa, D.; Nishi, H.; Kobatake, S. Photoinduced Twisting of a Photochromic Diarylethene Crystal. *Angew. Chem. Int. Ed.* **2013**, *52*, 9320-9322.

(13) Uchida, K.; Sukata, S. I.; Matsuzawa, Y.; Akazawa, M.; J. J. D. de Jong, Katsonis, N.; Kojima, Y.; Nakamura, S.; Areephong, J.; Meetsma, A.; Feringa, B. L. Photoresponsive Rolling and Bending of Thin Crystals of Chiral Diarylethenes. *Chem. Commun.* **2008**, 326-328.

(14) Kim, T.; Al-Muhanna, M. K.; Al-Suwaidan, S. D.; Al-Kaysi, R. O.; Bardeen, C. J. Photoinduced Curling of Organic Molecular Crystal Nanowires. *Angew. Chem. Int. Ed.* **2013**, *52*, 6889-6893.

(15) Al-Kaysi, R. O.; Tong, F.; Al-Haidar, M.; Zhu, L.; Bardeen, C. J. Highly Branched Photomechanical Crystals. *Chem. Commun.* **2017**, *53*, 2622-2625.

(16) Medishetty, R.; Sahoo, S. C.; Mulijanto, C. E.; Naumov, P.; Vittal, J. J. Photosalient Behavior of Photoreactive Crystals. *Chem. Mater.* **2015**, *27*, 1821-1829.

(17) Kitagawa, D.; Okuyama, T.; Tanaka, R.; Kobatake, S. Photoinduced Rapid and Explosive Fragmentation of Diarylethene Crystals Having Urethane Bonding. *Chem. Mater.* **2016**, *28*, 4889-4892.

(18) Naumov, P.; Sahoo, S. C.; Zakharov, B. A.; Boldyreva, E. V. Dynamic Single Crystals: Kinematic Analysis of Photoinduced Crystal Jumping (The Photosalient Effect). *Angew. Chem. Int. Ed.* **2013**, *52*, 9990-9995.

(19) Commins, P.; Natarajan, A.; Tsai, C.-K.; Khan, S. I.; Nath, N. K.; Naumov, P.; Garcia-Garibay, M. A. Structure−Reactivity Correlations and Mechanistic Understanding of the Photorearrangement and Photosalient Effect of α-Santonin and Its Derivatives in Solutions, Crystals, and Nanocrystalline Suspensions. *Cryst. Growth Des.* **2015**, *15*, 1983-1990.

(20) Tong, F.; Al-Haidar, M.; Zhu, L.; Al-Kaysi, R. O.; Bardeen, C. J. Photoinduced Peeling of Molecular Crystals. *Chem. Commun.* **2019**, *55*, 3709-3712.

(21) Cole, J. M.; Velazquez-Garcia, J. d. J.; Gosztola, D. J.; Wang, S. G.; Chen, Y.-S. Light-Induced Macroscopic Peeling of Single Crystal Driven by Photoisomeric Nano-Optical Switching. *Chem. Mater.* **2019**, *31*, 4927-4935.

(22) Hirano, A.; Kitagawa, D.; Kobatake, S. Photomechanical Bending Behavior of Photochromic Diarylethene Crystals Induced under Polarized Light. *CrystEngComm* **2019**, *21*, 2495-2501.

(23) Hirano, A.; Hashimoto, T.; Kitagawa, D.; Kono, K.; Kobatake, S. Dependence of Photoinduced Bending Behavior of Diarylethene Crystals on Ultraviolet Irradiation Power. *Cryst. Growth Des.* **2017**, *17*, 4819-4825.

(24) Kitagawa, D.; Tanaka, R.; Kobatake, S. Dependence of Photoinduced Bending Behavior of Diarylethene Crystals on Irradiation Wavelength of Ultraviolet Light. *Phys. Chem. Chem. Phys.* **2015**, *17*, 27300-27305.

(25) Kitagawa, D.; Iwaihara, C.; Nishi, H.; Kobatake, S. Quantitative Evaluation of Photoinduced Bending Speed of Diarylethene Crystals. *Crystals* **2015**, *5*, 551-561.

(26) Kitagawa, D.; Kobatake, S. Crystal Thickness Dependence of the Photoinduced Crystal Bending of 1-(5-Methyl-2-(4-(p-vinylbenzoyloxymethyl)phenyl)-4-thiazolyl)-2-(5-methyl-2-phenyl-4-thiazolyl)perfluorocyclopentene. *Photochem. Photobiol. Sci.* **2014**, *13*, 764-769.

(27) Kitagawa, D.; Kobatake, S. Crystal Thickness Dependence of Photoinduced Crystal Bending of 1,2-Bis(2-methyl-5-(4-(1-naphthoyloxymethyl)phenyl)-3-thienyl)perfluorocyclopentene. *J. Phys. Chem. C* **2013**, *117*, 20887-20892.

(28) Chizhik, S.; Sidelnikov, A.; Zakharov, B.; Naumov, P.; Boldyreva, E. Quantification of Photoinduced Bending of Dynamic Molecular Crystals: From Macroscopic Strain to Kinetic Constants and Activation Energies. *Chem. Sci.* **2018**, *9*, 2319-2335.

(29) Kim, T.; Zhu, L.; Mueller, L. J.; Bardeen, C. J. Mechanism of Photoinduced Bending and Twisting in Crystalline Microneedles and Microribbons Composed of 9-Methylanthracene. *J. Am. Chem. Soc.* **2014**, *136*, 6617-6625.

(30) Nath, N. K.; Pejov, L.; Nichols, S. M.; Hu, C.; Saleh, N.; Kahr, B.; Naumov, P. Model for Photoinduced Bending of Slender Molecular Crystals. *J. Am. Chem. Soc.* **2014**, *136*, 2757-2766.

(31) Kobatake, S.; Uchida, K.; Tsuchida, E.; Irie, M. Single-Crystalline Photochromism of Diarylethenes: Reactivity–Structure Relationship. *Chem. Commun.* **2002**, 2804-2805.

(32) Bravais, A. *Études Cristallographiques*, Paris: Gauthier-Villars, 1866.

(33) Friedel, G. Études sur la loi de Bravais. *Bull. Soc. Fr. Mineral.* **1907**, *30*, 326-455.

(34) Donnay, J. D. H.; Harker, D. A New Law of Crystal Morphology Extending the Law of Bravais. *Am. Mineral.* **1937**, *22*, 446-467.

(35) Kaminsky, W. From CIF to Virtual Morphology Using the WinXMorph Program. *J. Appl. Cryst.* **2007**, *40*, 382-385.

(36) Morimoto, M.; Kobatake, S.; Irie, M. Polymorphism of 1,2-Bis(2-methyl-5-*p*-methoxyphenyl-3-thienyl)perfluorocyclopentene and Photochromic Reactivity of the Single Crystals. *Chem. Eur. J.* **2003**, *9*, 621-627.

(37) Naumov, P.; Chizhik, S.; Panda, M. K.; Nath, N. K.; Boldyreva, E. Mechanically Responsive Molecular Crystals. *Chem. Rev.* **2015**, *115*, 12440-12490.

(38) Kobatake, S.; Kuratani, H. Photochromism of Diarylethene-Functionalized Polystyrene with High Conversion in a Solid-State Polymer Film. *Chem. Lett.* **2006**, *35*, 628-629.

Table of Contents